Design And Development of Wideband Antenna for Wireless and Bio-Medical Applications

SURENDRA LOYA[1], D.S.N. JYOTHI[2], K. GNANASAI[3], SD. JASMINE[4], E. HARSHA VARDHAN[5]
[1, 2, 3, 4, 5] *Department of ECE, Usha Rama College of Engineering and Technology*

Abstract— In this paper a wideband grounded co-planar waveguide-based patch antenna is designed. The proposed antenna is integrated with a slotted inverted delta-shaped main radiating patch, and co-planar waveguide elements and bottom of antenna partial ground with slots. The dimensions of antenna are 50x44x1.52mm^3. The designed antenna simulated and validated simulation results over a frequency range of 1.5-2.5GHZ.

I. INTRODUCTION

Due to developments in the wireless communications, there is a need to develop small scale antennas for transmitting and receiving data. The main disadvantages of CT scanning and X-ray imaging are dangerous radiation, relatively maximum false-negative percentage, lower susceptibility, growing cancerous hazard because of short dose [1], and ionizing radioactivity [2]. The utilisation of electronic devices increased day by day as per moors law. Refraction can produce challenges for medical imaging where some structures appear to be duplicated [5]. The small antennas can be used not only in wireless applications it can also be used in bio medical applications. The main aims of head imaging are to detect the presence and location of damaged brain tissues that are caused by different medical conditions or injuries, such as ischemic or haemorrhagic brain strokes [7]. This technology is compact and relatively cheap in comparison with conventional medical imaging techniques such as magnetic resonance imaging but recently the research has been extended to bone imaging and stroke detection in human head as well [9]. The proposed antenna can support for wireless technologies like phone, Bluetooth, Wi-Fi, ZigBee /IEEE 802.15.4 wireless data networks, RF peripherals, Audio-visual (AV) devices, Radio control. Although some existing imaging technologies, like CT and MRI, are capable of ICH diagnosis, they are time consuming, expensive, bulky and stationary [10]. In present day to treat the cancer we have different technologies like computed tomography (CT), PET (Positron emission tomography), Magnetic Resonance imaging (MRI), Ultrasound, X-ray imaging. These technologies are showing adverse effects on human body to treat the cancer and these technologies are more expensive and unhealthier, we proposed a microstrip slot antenna-based system for identification of tumour in head with the help of CST microwave studio.

II. ANTENNA DESIGN METHODOLOGY

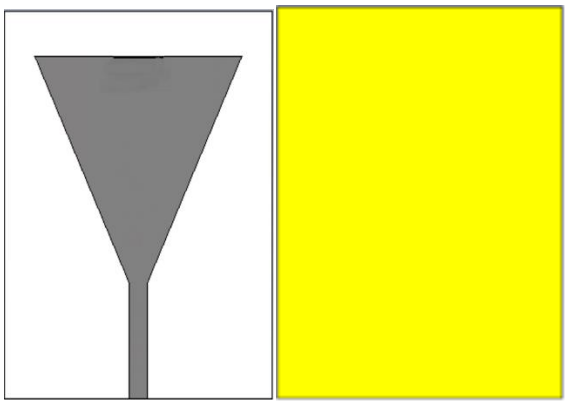

Front view Rear view

(a) Stage 1

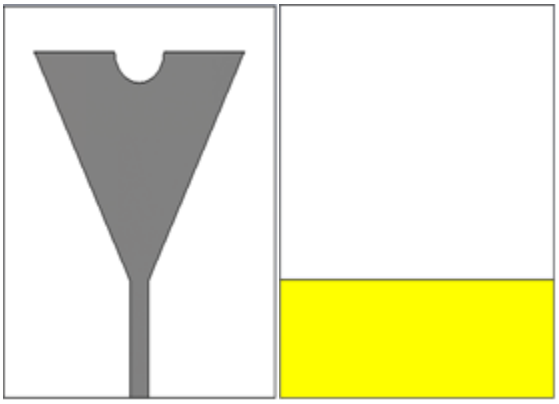

Front view Rear view

(b) Stage 2

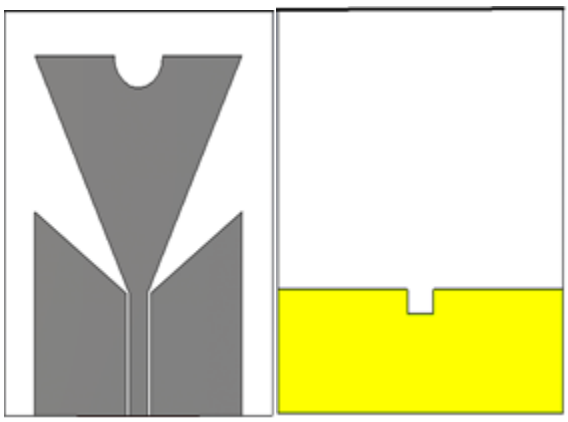

Front view Rear view

(c) Stage 3

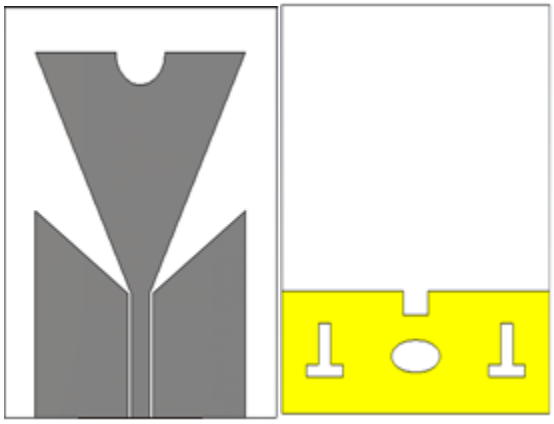

Front view Rear view

(d) Stage 4

Fig1: Antenna stage-wise front and back-view

Stage 1:

In the first stage, consider the substrate of FR4 with the parameters 50x44x1.52mm^3 by using CST software. Consider the ground under the substrate with the parameters as the substrate. Consider the main radiating patch over the substrate with parameters according to the geometrical model. Add the feed line to the main radiating patch. The material of patch and the ground is of copper.

Stage 2:

Take the partial ground from the full ground by cutting out the unwanted part of the ground.

Stage 3:

Now insert the semi-circle slot on the top of the main radiating patch according to the diameter given in the geo-metric table. Add the co-planar waveguide elements on either side of the feed line. Also consider the rectangular slot on the partial ground.

Stage 4:

In the final stage insert the elliptical shape and inverted-T shape slots on the ground and simulate the antenna by applying the field monitors. Observe the simulated results.

III. GEOMETRIC MODEL OF THE PROPOSED SYSTEM

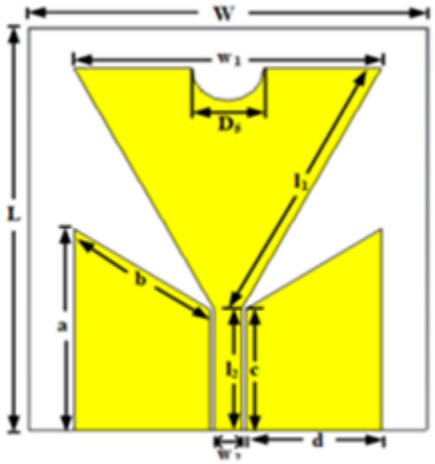

(a)

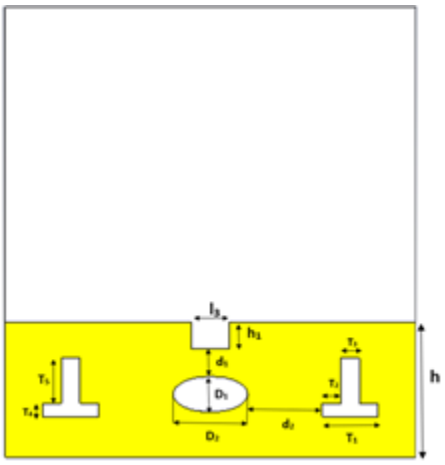

(b)

Fig 2: Geometric model of the proposed system: (a) Front view (b) Rear view

Figure 2 illustrates the geometrical construction with parameters notification of the antenna. The fabricated prototype is depicted in Figure 3.

IV. FABRICATED PHOTOGRAPH OF THE PROPOSED ANTENNA

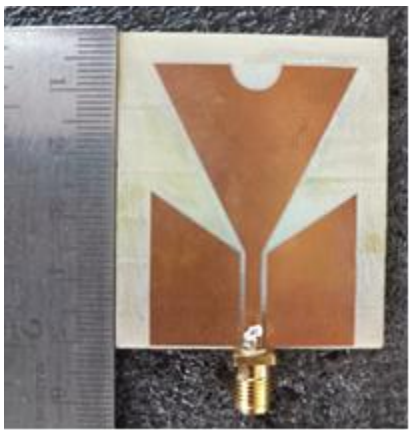

(a)

(b)

Fig 3: Fabricated photograph of the proposed antenna (a)Front view (b) Rear view

V. DESIGN EQUATIONS OF THE PROPOSED ANTENNA

$$w_1 = \frac{2c}{3f_r\sqrt{\varepsilon_r}}$$

$$\varepsilon_{e_{ff}} = \frac{(\varepsilon_r+1)}{2} + \frac{(\varepsilon_r-1)}{2}\left[1 + 10\frac{h}{w_1}\right]^{-\frac{1}{2}}$$

$$\Delta l = 0.415 \times \mathrm{h}\frac{(\varepsilon_{e_{ff}}+ 0.30)\,(\frac{w1}{h} + 0.26)}{(\varepsilon_{e_{ff}}- 0.258)(\frac{w1}{h} + 0.813)}$$

$$l_1 = \frac{2c}{3f_r\sqrt{\varepsilon_r}} - \Delta l$$

$$f_{lower} = \frac{c}{2 \times W_1\sqrt{\varepsilon_{e_{ff}}}}$$

Where as

ε_r is the dielectric constant of the substrate

h is the thickness of the substrate = 1.524 mm

f_{lower} is the lowest operating frequency of the antenna

$w_1$is the width of the patch

l_1 is the length of the side edge

c denotes the speed of light in open space

f_r is the resonance frequency

Δl is the normalized extension of the length of the patch

$\varepsilon_{e_{ff}}$ is the effective dielectric constant of the substrate

TABLE 1: All parameters of the proposed prototype

Parameters	Size(mm)	Parameters	Size(mm)
W	44	d_1	3
L	50	d_2	7
a	25	D_1	4
b	18.03	D_2	8
c	15	D_5	8
l_1	33.77	h_1	3
w_1	34	T_1	6
w_2	3	T_2	2
l_2	15	T_3	2
l_3	4	T_4	1.5
d	15	T_5	5
H	15		

In Table 1, 23 parameters are presented that are used to clarify the comprehensive prototype structure. Overall, the antenna's width and length are represented by W and L. The value of the parameters W and L are 44 mm and 50 mm respectively. The width of the top edge (patch width) and the length of the side edges of the slotted inverted delta-shaped radiating patch are represented by w_1 and l_1. The value of the parameters w_1 and l_1 are 34 mm and 33.77 mm respectively. One

half circle-shaped slot has been cut away at the central location of the top edge of the patch. Its diameter is denoted by D5 and value is considered as 8 mm. This shape changes the current movement on the top edge of the patch for increasing the radiation directivity. The width and length of the feed line are represented by w2 and l2. The value of the parameters w_2 and l_2 are 3 mm and 15 mm respectively. The feed line is electrically coupled with coplanar waveguide elements and the slotted bottom ground plane to enhance the matching of the input impedance of the antenna. After that, two coplanar waveguide elements are positioned alongside the feedline to increase the reflection coefficient under -10 dB, gain, as well as impedance matching. The arms of the two coplanar waveguide elements are denoted by a, b, c and d; and the values of the arms are considered as 25 mm, 18.03 mm, 15 mm, and 15 mm respectively. These values have an important impact on the S_{11} (refection coefficient) and the gain of the prototype. The width and length of the rectangular-shaped slot are represented by l_3 and h_1; as well as the value of the parameters l_3 and h_1 is 4 mm and 3 mm respectively. This shape slot has been cut away at the top-central location on the partial ground plane for decreasing the lower frequency, increase the refection coefficient under -10 dB, and enhance the gain of the prototype. Also, this changes the current movement path, inductance, and capacitance of the ground plane which are also helped to enhance the radiation directivity. A partial ground has been designed on the rear side of the substrate material. The length and width of the ground are represented by h and W. The considered value of the parameters h and W is 15 mm and 44 mm respectively. One elliptical-shaped slot and two inverted-T shaped slots have been cut out on the ground for a momentous effect on the radiation directivity, reflection coefficient, gain, and efficiency of the antenna. However, the distance d_1 between elliptical-shaped slot and inverted-T shaped slots is 7 mm and the distance d_2 between the middle rectangular-shaped slot and the middle elliptical slot is 3 mm. These distances have an important effect on the reflection coefficient and directivity of the radiation of the antenna. It is investigated that, if the distance values of d1 and d2 are gradually changed, then radiation directivity is changed due to improperly distributed of surface current on the ground. On the other hand, the y-diameter and x-diameter of the elliptical-shaped slot are represented by D_1 and D_2, as well as their considered values are 4 mm and 8 mm respectively. The dimensions of the inverted-T shaped slots are T_1, T_2, T_3, T_4 and T_5 are 6mm, 2 mm, 2mm, 1.5mm and 5mm respectively. These slots also helped to increase the S11 (reflection coefficient) below -10 dB, increase the gain, and increase the radiation directivity of the antenna owing to these shapes able to regulate the electromagnetic coupling influence among the patch, coplanar waveguide elements, and the partial bottom ground. As a result, improve the overall operating frequency band (1.70 GHz to 3.71 GHz) and other features of the proposed antenna prototype.

VI. RESULTS AND DISCUSSION

Performance of the proposed antenna is first verified via computer simulations. Next, the antenna is manufactured and tested to confirm its simulated performance. The software results observed in computer by simulation are S_{11} parameters, VSWR readings, Surface currents distribution and Gain of the antenna.

Software results:

I. S_{11} parameters:

S_{11} Means return loss it represents how much power is reflected from the antenna, and hence it is also called as the reflection coefficient.

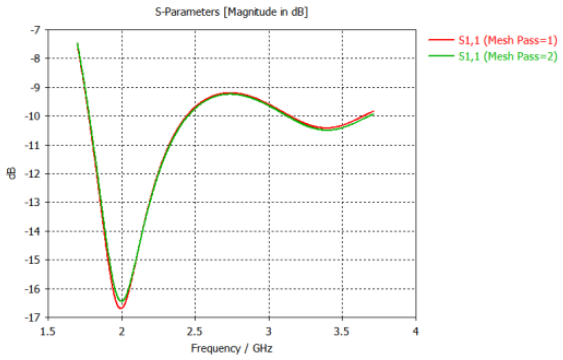

Fig 4: S_{11} parameters (reflection coefficient) of the proposed antenna

Our proposed antenna resonated between the frequency range of 1.7-3.71 GHz. We got dual band in frequency range 1.7-2.4 GHz and 3.1-3.71 GHz. In the first frequency band the antenna maximum resonated

at 2GHz and in the second band maximum resonance at 3.4GHz frequency. So, we have to consider the simulation results at the frequency 2 GHz and 3.4GHz.

II. VSWR measurements:

Voltage Standing Wave Ratio is a measure of how efficiently radio power is transmitted from a power source through a transmission line.

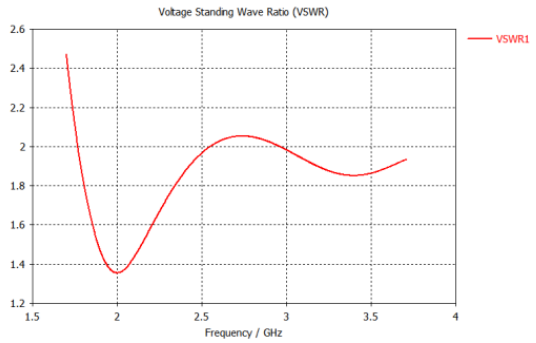

Fig 5: VSWR of the proposed antenna

The VSWR measurements of proposed antenna must be below the 2 for the better performance.

III. E-fields:

Electromagnetic waves are made up of electric fields coefficient called the E-field. An electric field is the physical field that surrounds electrically charged particles and exerts force on all other charged particles in the field, either attracting or repelling them. It also refers to the physical field for a system of charged particles.

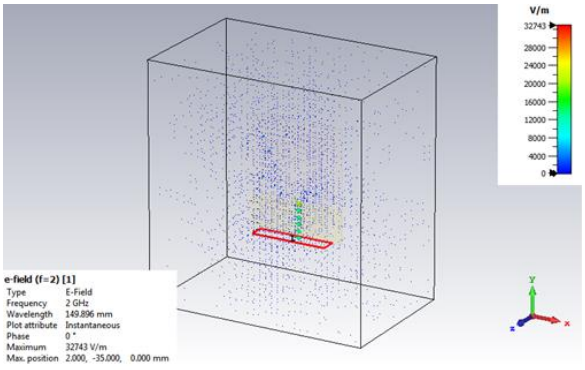

(a)

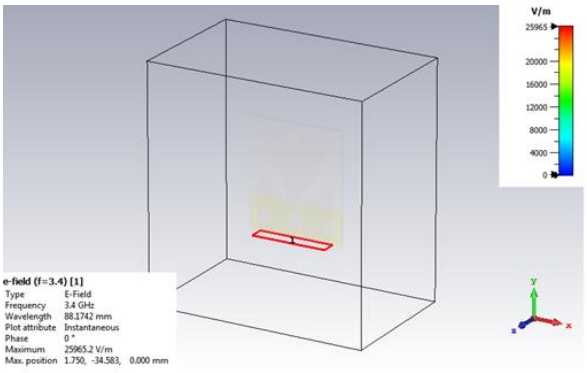

(b)

Fig 6: E-fields (a) at 2GHz and (b) at 3.4GHz

According to the resonated frequency we have to consider the E-fields. At maximum resonance frequency 2GHz and second band resonated frequency 3.4GHz the values are considered above in the scale.

IV. H-fields:

Electromagnetic waves are made up of electrical fields and magnetic fields and also called as H-field.

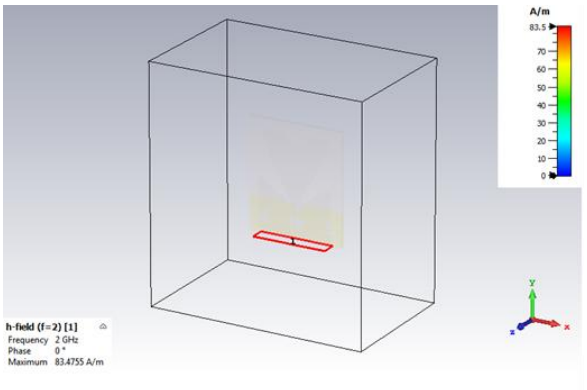

(a)

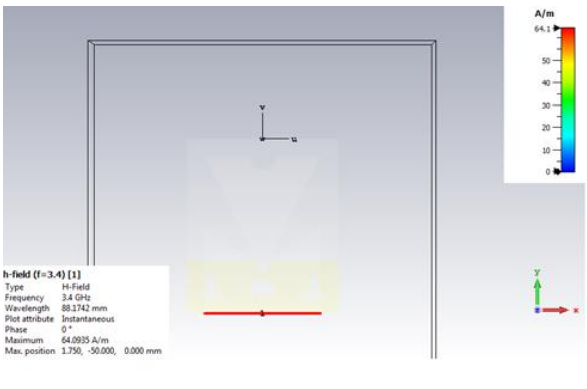

(b)

Fig 7: H-fields (a) at 2GHz and (b) at 3.4GHz

According to the resonated frequency we have to consider the H-fields. At maximum resonance frequency 2GHz and second band resonated frequency 3.4GHz the values are considered above in the scale.

VII. SURFACE CURRENT DISTRIBUTION

Surface current is a current flowing in a plane, and has units of charge per unit time per unit length (measured in the direction in the same plane but perpendicular to the flow direction). The below figures give the values of distribution of surface currents at 2GHz frequency and 3.4 GHz frequency. Figure a represents the surface current distribution at 2GHz frequency and figure b represents the surface current distribution at 3.4GHz frequency.

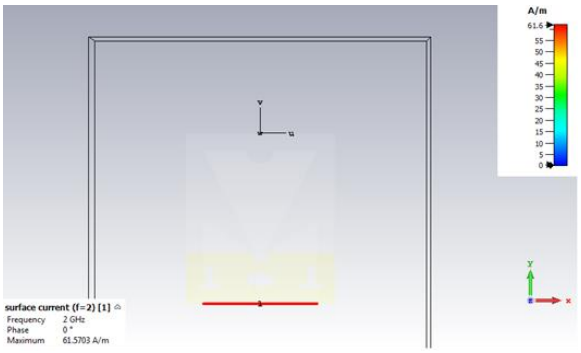

(a)

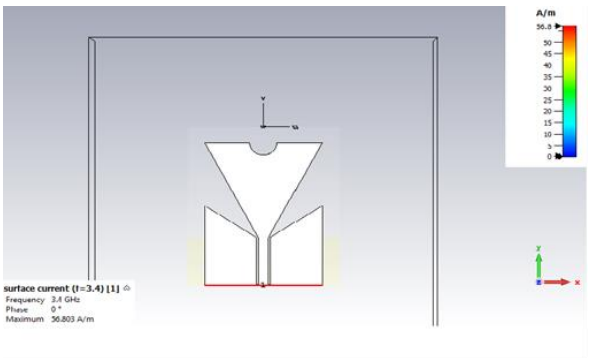

(b)

Fig 8: Surface current distribution (a) at 2GHz and (b) at 3.4GHz

VIII. DIRECTIVITY OF THE PROPOSED ANTENNA

Directivity is a parameter of an antenna or optical system which measures the degree to which the radiation emitted is concentrated in a single direction. It is the ratio of the radiation intensity in a given direction from the antenna to the radiation intensity averaged over all directions.

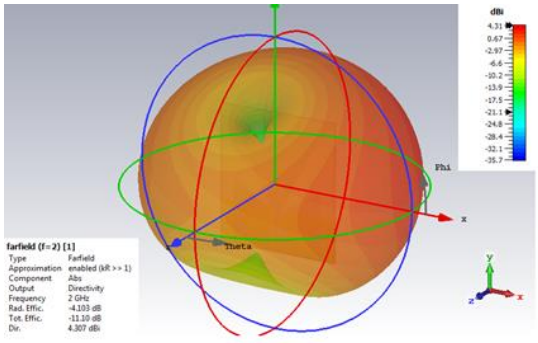

(a)

Figure 9 represents the directivity of the proposed antenna in polar and 3D pattern at 2GHz frequency. The directivity of the antenna is shown in the above figure and the directivity at 2GHz is 2.364dBi.

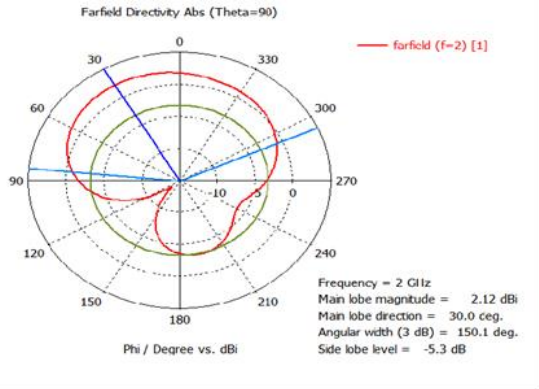

(b)

Fig 9: Directivity of the antenna at 2GHz (a) 3D and (b) 2D

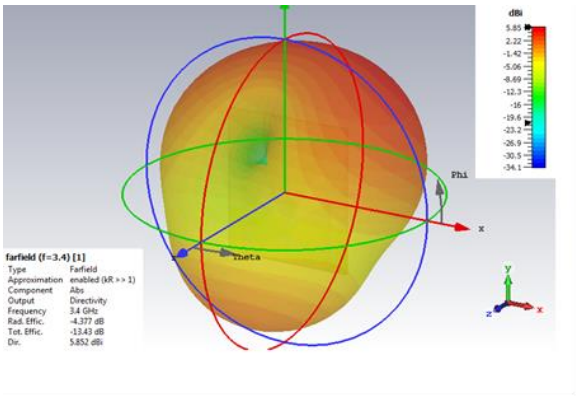

(a)

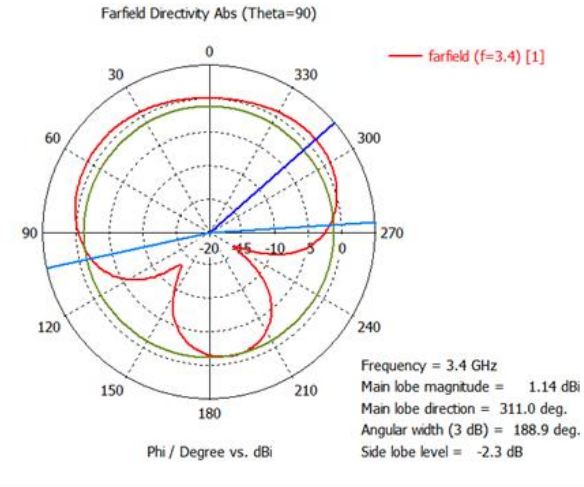

(b)

Fig 10: Directivity of the antenna at 3.4GHz (a) 3D and (b) 2D

Figure 10 represents the directivity of the proposed antenna in polar and 3D pattern at 3.4GHz frequency. The directivity of the antenna is shown in the above figure and the directivity at 3.4GHz is 2.127dBi.

Hardware results:

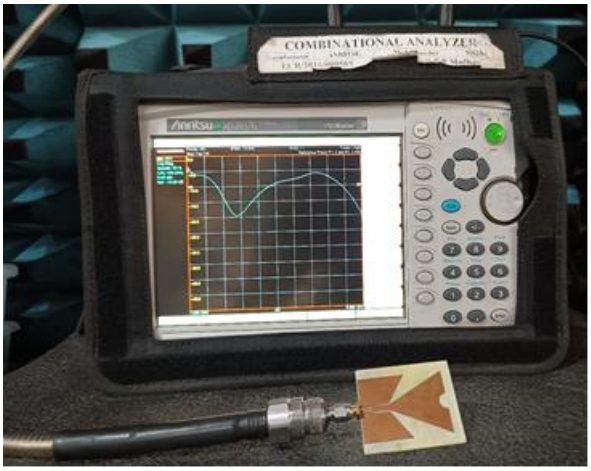

Fig 11: Network Analyzer for the proposed Antenna

A network analyser is an instrument that measures the network parameters of electrical networks. Today, network analysers commonly measure s–parameters because reflection and transmission of electrical networks are easy to measure at high frequencies, but there are other network parameter sets such as y-parameters, z-parameters, and h-parameters. Network analysers are often used to characterize two-port networks such as amplifiers and filters, but they can be used on networks with an arbitrary number of ports.

IX. APPLICATION OF THE PROPOSED ANTENNA IN THE HEAD IMAGING

A human head consists of six tissue layers such as skin, fat, bone or skull, CSF (cerebral spinal fluid), grey matter, and white matter. The brain of the head is combined by both grey and white matter. This simulation is performed in three dimensional (3D) CST 2019 software. The hemisphere model with the general structure of the head is illustrated. The antenna is placed 15 mm away from the skin layer of the hemisphere head model

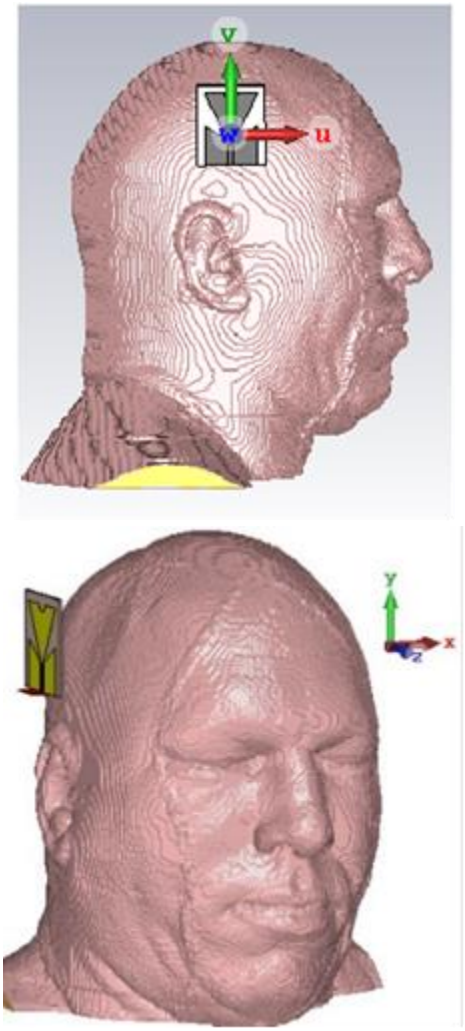

Fig 12: Hugo head model with single antenna.

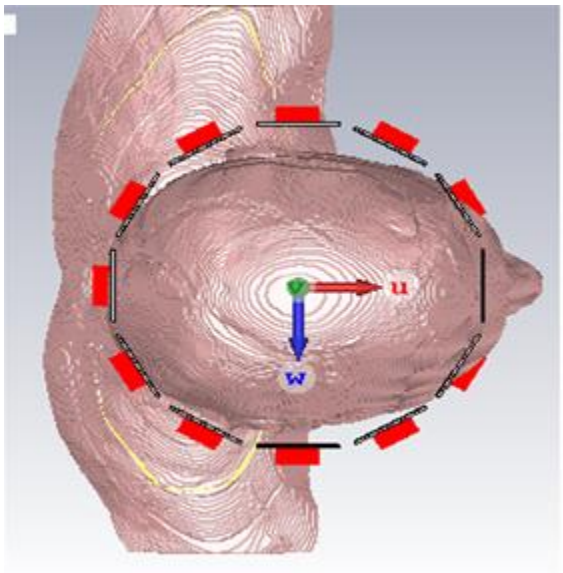

Fig 13: Proposed antenna arrays simulation with head phantom Model with 12 antenna arrays set up top view

TABLE 2: Different tissues of the Hugo head model

Name of the Tissues	Thickness (mm)
Skin	0.5-1.5
Fat	1
Skull	3-11
CSF	0.5
Gray matter	7
White matter	Internal part

Above table represents the six layers of the Hugo head model and the thickness of the layers in mm. The thickness of the Skin is from 0.5-1.5, and the thickness of the Fat is 1, and the thickness of the Skull is from 3-11, and the thickness of the CSF is 0.5, and the thickness of the Gray matter is 7, and the thickness of the White matter is Internal part.

The proposed antenna can also be used for the detection of tumor in the human body. The array of antennas arranged around the part of the body which was affected with the tumor. Proposed antenna is not only for the wireless communication but also for the bio-medical applications. This Bio-medical application can also be implemented by using 3-D CST Studio software and can simulate to observe the results.

CONCLUSION

The proposed antenna is showing good band width and it is operating in the band 1.7-2.4 GHz and 3.1-3.71 GHz and observed the antenna parameters like S11, VSWR, Directivity, Far Fields, E-plane, H-plane, Surface currents etc... This antenna is also proposed for bio medical applications like head imaging. The simulated and fabricated measured results are similar in the design and the proposed antenna is good candidate for wireless applications.

REFERENCES

[1] K. Kerlikowske, C. C. Gard, B. L. Sprague, J. A. Tice, and D. L. Miglioretti, ``One versus two breast density measures to predict 5-and 10-year

breast cancer risk," Cancer Epidemiol. Biomarkers Prevention, vol. 24, no. 6, pp. 889_897, Jun. 2015.

[2] H. Been Lim, N. Thi Tuyet Nhung, E.-P. Li, and N. D. Thang, ``Confocal microwave imaging for breast cancer detection: Delay-multiply-and-sum image reconstruction algorithm," IEEE Trans. Biomed. Eng., vol. 55, no. 6, pp. 1697_1704, Jun. 2008.

[3] M. A. Jacobs, T. S. Ibrahim, and R. Ouwerkerk, ``MR imaging: Brief overview and emerging applications," RadioGraphics, vol. 27, no. 4,pp. 1213_1229, Jul. 2007.

[4] P. A. T. Baltzer, M. Benndorf, M. Dietzel, M. Gajda, I. B. Runnebaum, and W. A. Kaiser, ``False-positive _ndings at contrast-enhanced breast MRI: A BI-RADS descriptor study," Amer. J. Roentgenol., vol. 194, no. 6, pp. 1658_1663, Jun. 2010.

[5] V. Chan and A. Perlas, ``Basics of ultrasound imaging," in Atlas of Ultrasound-Guided Procedures in Interventional Pain Management. New York, NY, USA: Springer-Verlag, 2011, pp. 13_19.

[6] M. S. R. Bashri, T. Arslan, and W. Zhou, ``Flexible antenna array for wearable head imaging system," in Proc. 11th Eur. Conf. Antennas Propag. (EUCAP), Mar. 2017, pp. 172_176.

[7] B. J. Mohammed, A. M. Abbosh, S. Mustafa, and D. Ireland, ``Microwave system for head imaging," IEEE Trans. Instrum. Meas., vol. 63, no. 1, pp. 117_123, Jan. 2014.

[8] S. Ahdi Rezaeieh, A. Zamani, K. S. Bialkowski, and A. M. Abbosh, ``Foam embedded wideband antenna array for early congestive heart failure detection with tests using articular phantom with animal organs," IEEE Trans. Antennas Propag., vol. 63, no. 11, pp. 5138_5143, Nov. 2015.

[9] M. Jalilvand, T. Zwick, W. Wiesbeck, and E. Pancera, ``UWB synthetic aperture-based radar system for hemorrhagic head-stroke detection," in Proc. IEEE RadarCon (RADAR), May 2011, pp. 956_959.

[10] A. T. Mobashsher and A. M. Abbosh, ``On-site rapid diagnosis of intracranial hematoma using portable multi-slice microwave imaging system," Sci. Rep., vol. 6, no. 1, p. 37620, Dec. 2016.

[11] A. Hossain, M. T. Islam, A. F. Almutairi, M. S. J. Singh, K. Mat, andM. Samsuzzaman, ``An octagonal ring-shaped parasitic resonator based compact ultrawideband antenna for microwave imaging applications," Sensors, vol. 20, no. 5, p. 1354, Mar. 2020.

[12] I. Saied and T. Arslan, ``Microwave imaging algorithm for detecting brain disorders," in Proc. 29th Int. Conf. Radioelektronika (RADIOELEKTRON-IKA), 2019, pp. 1_5.

[13] A. T. Mobashsher, A. M. Abbosh, and Y. Wang, ``Microwave system to detect traumatic brain injuries using compact unidirectional antenna and wideband transceiver with veri_cation on realistic head phantom," IEEE Trans. Microw. Theory Techn., vol. 62, no. 9, pp. 1826_1836, Sep. 2014.

[14] A. T. Mobashsher, K. S. Bialkowski, and A. M. Abbosh, ``Design of compact cross-fed three-dimensional slot-loaded antenna and its application in wideband head imaging system," IEEE Antennas Wireless Propag. Lett., vol. 15, pp. 1856_1860, 2016.

[15] A. T. Mobashsher and A. Abbosh, ``Slot-loaded folded dipole antenna with wideband and unidirectional performance for L-band applications," IEEE Antennas Wireless Propag. Lett., vol. 13, pp. 798_801, 2014.

[16] B. Sohani, G. Tiberi, N. Ghavami, M. Ghavami, S. Dudley, and Rahmani, ``Microwave imaging for stroke detection: Validation on head-mimicking phantom," in Proc. Photon. Electromagn. Res. Symp. Spring (PIERS-Spring), Jun. 2019, pp. 940_948.

[17] M. Ojaroudi, S. Bila, and M. Salimi, ``A novel approach of brain tumor detection using miniaturized high-_delity UWB slot antenna array," in Proc. 13th Eur. Conf. Antennas Propag. (EuCAP), 2019, pp. 1_5.